Anomalous surface conductivity of Weyl semimetals

Hridis K. Pal,[1] Osakpolor Eki Obakpolor [●],[2] and Pavan Hosur [●][2]

[1]*Department of Physics, Indian Institute of Technology Bombay, Powai, Mumbai 400076, India*
[2]*Department of Physics, University of Houston, Houston, Texas 77204, USA*

We calculate the surface dc conductivity of Weyl semimetals and show that it contains an anomalous contribution in addition to a Drude contribution from the Fermi arc. The anomalous part is independent of the surface scattering time, and appears at nonzero temperature and doping (away from the Weyl nodes), increasing quadratically with both with a universal ratio of coefficients. Microscopically, it results from the contribution of the gapless bulk to the surface conductivity. We argue that this can be interpreted as the conductivity of an effective interacting surface fluid that coexists with the Fermi arc metal. In a certain regime of low temperatures, the temperature dependence of the surface conductivity is dominated by the anomalous response, which can be probed experimentally to unravel the unusual behavior.

I. INTRODUCTION

Weyl semimetals (WSMs) are gapless topological materials defined by nondegenerate bands in the bulk intersecting at isolated points in the momentum space [1–18]. These points, known as Weyl nodes, have a well-defined chirality and host quasiparticles that mimic relativistic Weyl fermions first studied in high-energy physics. Since Weyl fermions are topological objects, their response to external electromagnetic fields is distinct from that of usual Bloch electrons in conventional solids. Numerous such bulk topological responses have been extensively investigated, both in theory and in experiments, over the past decade [19–39].

The surface of a WSM, however, has remained more mysterious. It hosts unusual metallic states known as Fermi arcs (FAs) that connect surface projections of bulk Weyl nodes of opposite chiralities. They do not form a closed contour, unlike Fermi surfaces in conventional two-dimensional (2D) metals [8–16,40–58]. This raises the possibility of unusual response on the surface to external electromagnetic fields [59–63]. However, investigations in this direction are rendered challenging by the fact that at the end points of the FAs, the wave function merges with the bulk Bloch waves at the Weyl nodes and renders the surface of a WSM fundamentally inseparable from the bulk. This is in stark contrast to the surface states of topological insulators, which decay exponentially into the bulk at all surface momenta [64,65]. The bulk-surface inseparability in WSMs can also be understood from an energy-based perspective. Since a topological insulator is gapped in the bulk, its low-energy theory consists of a strictly surface Hamiltonian. In contrast, WSMs have gapless states both in the bulk and on the surface, so an energy cutoff is not available to disentangle the surface from the bulk. While the surface-bulk inseparability promises rich physics such as quantum oscillations from cyclotron orbits composed of FAs and chiral modes in the bulk [55–58,66–70],

unusual collective modes [71–79], and dissipative chiral transport [59], it invalidates a strictly surface Hamiltonian, thereby hindering a controlled theoretical description of the surface and leaving its electromagnetic response poorly understood.

In this work, we calculate a basic surface transport property of a WSM, namely, the dc conductivity σ_{surf}. Unlike previous studies of surface transport in WSMs that exclusively focus on the contributions of the FAs [59–63], we include the nontrivial influence of the bulk on the surface in a controlled manner and show that σ_{surf} is comprised of two qualitatively different contributions:

$$\sigma_{\text{surf}} = \sigma_{\text{norm}} + \sigma_{\text{anom}}. \tag{1}$$

Here, σ_{norm} is a normal, Drude-like conductivity arising from the FA. It is proportional to the scattering time (τ) and has a negligible dependence on temperature (T) besides the T dependence of τ. In contrast, σ_{anom} is an anomalous term arising from the bulk states. It is τ independent, but has a characteristic dependence on both T and doping around the Weyl nodes, μ: $\sigma_{\text{anom}} \propto \mu^2 + k_B^2 T^2 \pi^2/3$. Crucially, the coefficients have a universal ratio, $k_B^2 \pi^2/3$, independent of material parameters. In a regime of low temperatures described later, the T-dependent part of σ_{surf} is dominated by σ_{anom}, which provides immediate experimental access to σ_{anom}. Note that σ_{anom} is τ independent even if the bulk quasiparticles have a nonzero lifetime. This is reminiscent of the universal minimal conductivity of a 2D Dirac fermion that only depends on fundamental constants [80]. As espoused later, the electrical response of the bulk states on the surface mimics that of an interacting 2D fluid that coexists with the FA metal on the surface. This, in turn, gives rise to unusual form of σ_{anom} in Eq. (1). Thus, the daunting problem of the 2D FAs coexisting with the 3D bulk states reduces to a tractable, strictly 2D, effective two-fluid problem.

II. MODEL

We employ a variant of the model introduced in Ref. [44] for generating a WSM with arbitrary configurations of FAs and Weyl nodes. The model consists of a finite stack of metallic bilayers whose Hamiltonian as a function of $\mathbf{k} = (k_x, k_y)$ is

$$
H_{\mathbf{k}} = \sum_{z=1}^{L} \psi_{z,\mathbf{k}}^{\dagger}[(-1)^z \xi_{\mathbf{k}} - \mu]\psi_{z,\mathbf{k}}
$$
$$
- \sum_{z=1}^{L-1} \psi_{z,\mathbf{k}}^{\dagger} t_{z,\mathbf{k}} \psi_{z+1,\mathbf{k}} + \text{H.c.}, \qquad (2)
$$

where $\psi_{z,\mathbf{k}}^{\dagger}$ creates an electron with momentum $\hbar\mathbf{k}$ in layer z, $\xi_{\mathbf{k}}$ denotes a metallic dispersion with Fermi surface along $\xi_{\mathbf{k}} = 0$, μ is the bulk chemical potential and the interlayer hopping modulates as $t_{z,\mathbf{k}} = t_{\perp} + (-1)^z \delta t_{\mathbf{k}}$. If $|\delta t_{\mathbf{k}}| < |t_{\perp}| \ \forall \ \mathbf{k}$, $H_{\mathbf{k}}$ produces bulk Weyl nodes in the $k_z = \pi/2c$ plane, where $2c$ is the lattice constant along z, at discrete points $\mathbf{K}_j \equiv (K_{jx}, K_{jy})$ such that $\xi_{\mathbf{K}_j} = \delta t_{\mathbf{K}_j} = 0$. Near the jth node, the bulk Hamiltonian is $H_{\text{Weyl},j}(\mathbf{q}) = \hbar\mathbf{q} \cdot (\mathbf{v}_j \sigma_z + \mathbf{u}_j \sigma_x + \mathbf{w}_j \sigma_y) - \mu$, where σ_α are bilayer Pauli matrices and $\mathbf{v}_j = \frac{1}{\hbar}\nabla_{\mathbf{K}_j}\xi_{\mathbf{K}_j}$, $\mathbf{u}_j = \frac{2}{\hbar}\nabla_{\mathbf{K}_j}\delta t_{\mathbf{K}_j}$, and $\mathbf{w}_j = -\frac{2}{\hbar}t_{\perp}c\hat{\mathbf{z}}$ are Weyl velocities.

The surface ($z = 1$) Matsubara Green's function in the clean, noninteracting limit when $L \to \infty$ is [44,81] (see Supplemental Material [SM] [82] for details)

$$
G_{\mathbf{k}}(iE_n) = \frac{a_{\mathbf{k}}(iE_n) + b_{\mathbf{k}}(iE_n)}{2(t_{\perp} + \delta t_{\mathbf{k}})^2(iE_n + \mu - \xi_{\mathbf{k}})},
$$
$$
a_{\mathbf{k}}(iE_n) = (iE_n + \mu)^2 - \xi_{\mathbf{k}}^2 + 4t_{\perp}\delta t_{\mathbf{k}},
$$
$$
b_{\mathbf{k}}(iE_n) = \sqrt{\prod_{\lambda=\pm}\left[(iE_n + \mu)^2 - E_{\mathbf{k}\lambda}^2\right]}, \qquad (3)
$$

where $E_{\mathbf{k}+} = \sqrt{\xi_{\mathbf{k}}^2 + 4t_{\perp}^2}$ and $E_{\mathbf{k}-} = \sqrt{\xi_{\mathbf{k}}^2 + 4\delta t_{\mathbf{k}}^2}$ are the extremities of the bulk conduction band at $\mathbf{k}$. For real energies, $G_{\mathbf{k}}(E)$ has BCs when $|E + \mu| \in [E_{\mathbf{k}-}, E_{\mathbf{k}+}]$, i.e., E lies within the bulk bands, which we dub the BC region. When $|E + \mu| \notin [E_{\mathbf{k}-}, E_{\mathbf{k}+}]$, dubbed the N region, $G_{\mathbf{k}}(E)$ has simple poles along $E = \xi_{\mathbf{k}} - \mu$ when $t_{\perp}\delta t_{\mathbf{k}} > 0$ that define the FAs (Fig. 1). Importantly, the poles and BCs are generic features of surface Green's functions in WSMs and are not specific to the current model [81].

III. SURFACE CONDUCTIVITY

Since our goal here is to investigate surface transport, we need to introduce a nonzero quasiparticle lifetime $\tau_{\mathbf{k}}$ into Eq. (3) that captures the effect of scattering required to relax momentum gained due to the external field. To this effect, we revisit Eq. (2): A nonzero lifetime is introduced in each layer and the surface ($z = 1$) Matsubara Green's function is reevaluated, see SM [82] for details. We assume scattering to be weak such that $1/\tau_{\mathbf{k}} \to 0$. Analytically continuing, the

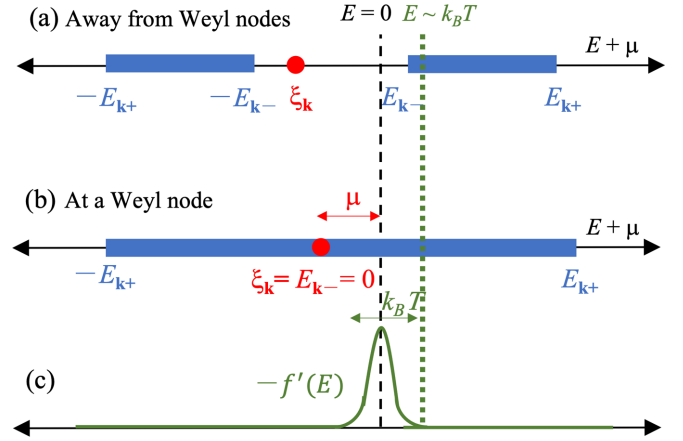FIG. 1. Schematic of contributions to σ_{anom}. Red dots (blue bars) denote the pole (BCs) of $G_{\mathbf{k}}(E)$ and physically represent the FA (bulk) states. (a) Away from the Weyl nodes, the BCs do not contain $E = 0$, resulting in no contribution to σ_{anom} (b) At a Weyl node, $\xi_{\mathbf{k}} = E_{\mathbf{k}-} = 0$, so both BCs touch the pole and $E = 0$ lies within one of them, which results in a nonzero σ_{anom} governed by μ. (c) $T \neq 0$ leads to σ_{anom} by enabling access to states within a BC via broadening of $-\partial_E f$.

retarded Green's functions in the N and BC regions are found to be

$$
G_{\mathbf{k}}^{R}(E) = \frac{a_{\mathbf{k}}(E) + b_{\mathbf{k}}(E)}{2(t_{\perp} + \delta t_{\mathbf{k}})^2\left(E + \mu - \xi_{\mathbf{k}} + \frac{i\hbar}{2\tau_{\mathbf{k}}}\right)}, E \in N \quad (4)
$$
$$
G_{\mathbf{k}}^{R}(E) = \frac{a_{\mathbf{k}}(E) + i\,\text{sgn}(E + \mu)|b_{\mathbf{k}}(E)|}{2(t_{\perp} + \delta t_{\mathbf{k}})^2\left(E + \mu - \xi_{\mathbf{k}} + \frac{i\hbar}{2\tau_{\mathbf{k}}}\right)}, E \in BC. \quad (5)
$$

Note that we have assumed only E-independent scattering processes for simplicity, but relaxing this assumption will not change our qualitative results.

The longitudinal dc conductivity along x direction due to the motion of electrons only on the surface is given by

$$
\sigma_{\text{surf}} = \frac{e^2\hbar}{2}\int_{E,\mathbf{k}}\left(-\frac{\partial f}{\partial E}\right)[v_{\mathbf{k},x}A_{\mathbf{k}}(E)]^2, \qquad (6)
$$

where $f(E) = 1/[1 + \exp(E/k_B T)]$, $\int_{E,\mathbf{k}} = \int \frac{d^2k\,dE}{(2\pi)^3}$, $v_{\mathbf{k},x} = \frac{1}{\hbar}\partial_{k_x}\xi_{\mathbf{k}}$ is the x component of the in-plane velocity, and $A_{\mathbf{k}}(E) = -2\text{Im}G_{\mathbf{k}}^{R}(E)$ is the surface spectral function. Due to the distinct forms of $G_{\mathbf{k}}^{R}(E)$ in the N and BC regions, it is convenient to split the E integral as $\int_E = \int_{E\in N} + \int_{E\in BC} \equiv \int_N + \int_{BC}$. The two terms yield σ_{norm} and σ_{anom}, respectively, which leads to the decomposition of σ_{surf} stated in Eq. (1). Moreover, in the limit $1/\tau_{\mathbf{k}} \to 0$, $\int_N$ receives contributions only from a sharp quasiparticle peak in $A_{\mathbf{k}}(E)$ due to the FAs while $\int_{BC}$ depends only on a broad feature in $A_{\mathbf{k}}(E)$ that captures the surface projection of the bulk states. Thus, σ_{norm} and σ_{anom} are in one-to-one correspondence with the FA and the bulk contributions to surface transport.

In the N-region, Eqs. (3), (4), and (6) give $A_{\mathbf{k}}(E) = 2\pi W_{\mathbf{k}}\delta_{\hbar/2\tau_{\mathbf{k}}}(E + \mu - \xi_{\mathbf{k}})$, where $W_{\mathbf{k}} = R[\frac{4t_{\perp}\delta t_{\mathbf{k}}}{(t_{\perp} + \delta t_{\mathbf{k}})^2}]$ with $R(x) = x\Theta(x)$ and $\delta_\eta(x) = \frac{1}{\pi}\frac{x}{x^2 + \eta^2}$. For $1/\tau_{\mathbf{k}} \to 0$, Eq. (6)

then yields,

$$\sigma_{\text{norm}} = e^2 \int_N \left(-\frac{\partial f}{\partial E} \right) \int_{\mathbf{k}} 2\pi \tau_{\mathbf{k}} v_{\mathbf{k},x}^2 W_{\mathbf{k}}^2 \delta(E + \mu - \xi_{\mathbf{k}}). \quad (7)$$

The factor $W_{\mathbf{k}}^2$ above ensures that σ_{norm} gets contributions only from the metallic FAs. Additionally, the contribution varies as one traverses the FA: It is largest near the middle of the FA (maximum $t_\perp \delta t_{\mathbf{k}}$), vanishes at the Weyl nodes ($\delta t_{\mathbf{k}} = 0$), and remains zero in regions lacking FAs ($t_\perp \delta t_{\mathbf{k}} < 0$). At $T = 0$, we find

$$\sigma_{\text{norm}} = 2e^2 \nu_F D, \quad (8)$$

where $\nu_F = \int_{\mathbf{k}} W_{\mathbf{k}} \delta(\mu - \xi_{\mathbf{k}})$ and $D = \frac{1}{2} \langle v_{F,x}^2 \tau \rangle = (2\nu_F)^{-1} \int_{\mathbf{k}} \delta(\mu - \xi_{\mathbf{k}})(v_{\mathbf{k},x} W_{\mathbf{k}})^2 \tau_{\mathbf{k}}$ are the suitably weighted means of the density of states per unit area (DOS) and the diffusion constant due to the FAs. Clearly, σ_{norm} is the Drude conductivity, scaling linearly with τ. At nonzero T, temperature enters the conductivity mainly through $\tau_{\mathbf{k}}$, which is model dependent, and is discussed later. Temperature may also enter via corrections to the DOS arising from the Sommerfeld expansion. However, such corrections vanish exactly for an ordinary 2D parabolic dispersion. By extension, the corrections are expected to be small for generic 2D metals including the FA metal, which we ignore henceforth.

In the BC region, Eqs. (3), (5), and (6) give the anomalous contribution to the conductivity:

$$\sigma_{\text{anom}} = 2e^2 \hbar \int_{BC} \left(-\frac{\partial f}{\partial E} \right) \int_{\mathbf{k}} v_{\mathbf{k},x}^2 \times$$
$$\frac{\left[(E + \mu)^2 - E_{\mathbf{k}-}^2 \right]\left[E_{\mathbf{k}+}^2 - (E + \mu)^2 \right]}{(E + \mu - \xi_{\mathbf{k}})^2 (t_\perp + \delta t_{\mathbf{k}})^2}. \quad (9)$$

At low T, $f'(E)$ restricts E to within $\pm \mathcal{O}(k_B T)$, so the BC region effectively obeys $E_{\mathbf{k}-} \lesssim k_B T + |\mu| \lesssim E_{\mathbf{k}+}$. Now, $E_{\mathbf{k}-} \geqslant 0 \; \forall \; \mathbf{k}$ and vanishes only at the Weyl nodes, where the bulk bands touch. As a result, the dominant contribution to σ_{anom} comes from the vicinity of the Weyl nodes. Thus, we can linearize around the jth node as $\xi_{\mathbf{k}} \approx \hbar \mathbf{v}_j \cdot \mathbf{q}$ and $\delta t_{\mathbf{k}} \approx \frac{\hbar}{2} \mathbf{u}_j \cdot \mathbf{q}$. Eq. (9) then evaluates to (see SM [82] for details)

$$\sigma_{\text{anom}} = \frac{e^2 c}{\hbar^2 \pi^2} \sum_j \left(\mu^2 + \frac{k_B^2 T^2 \pi^2}{3} \right) \frac{v_{j,x}^2}{t_\perp |(\mathbf{u}_j \times \mathbf{v}_j) \cdot \mathbf{w}_j|}, \quad (10)$$

where we assumed $|\mu|, k_B T \ll t_\perp$. If the Weyl nodes are at different energies, we must replace $\mu \to \mu_j$, the chemical potential relative to the energy of the jth node. A remarkable feature of σ_{anom} is that it is independent of τ, the in-plane scattering time. Thus, σ_{anom} manifestly has a different origin and expression compared to the Drude contribution, σ_{norm}. An exact numerical calculation of Eq. (6), shown in Fig. 2, corroborates our analytical results for both the Drude as well as the anomalous conductivities.

IV. EFFECTIVE INTERACTING SURFACE FLUID

We now reinterpret σ_{anom} as the conductivity of an effective interacting surface fluid. To this end, we consider the surface particle density at $1/\tau_{\mathbf{k}} \to 0$, $n = \int_{\mathbf{k},E} A_{\mathbf{k}}(E) = n_{\text{norm}} + n_{\text{anom}}$

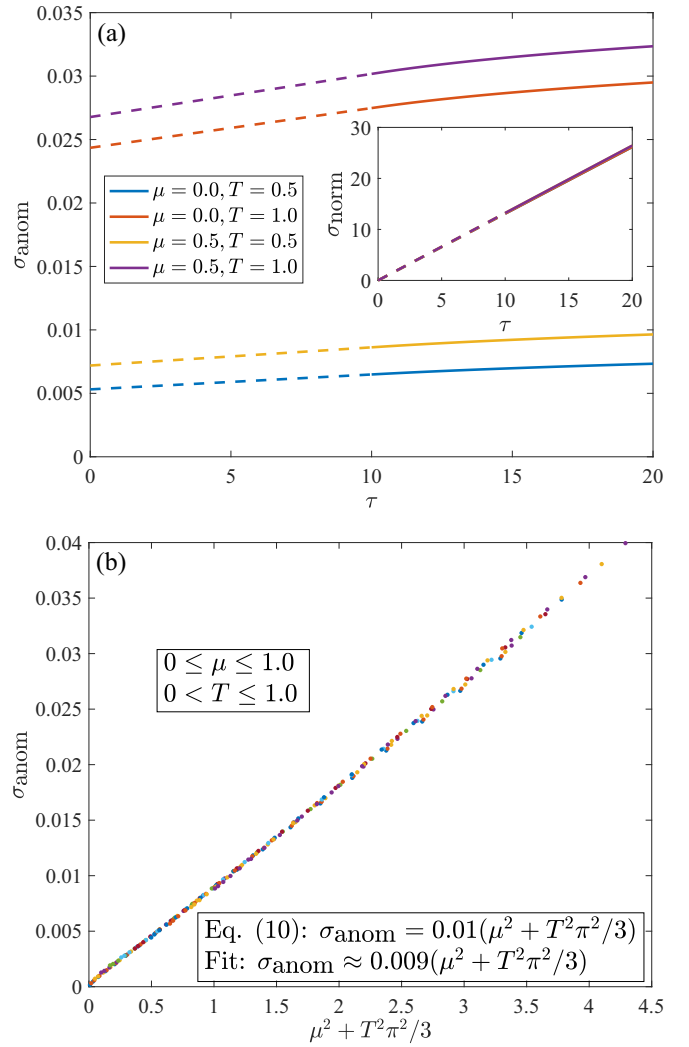FIG. 2. σ_{anom} and σ_{norm} calculated numerically from Eq. (6) by separating the pole and BC contributions to $A_{\mathbf{k}}(E)$ and assuming a $\mathbf{k}$-independent lifetime τ for simplicity. (a) σ_{anom} is nearly τ independent and has a finite intercept when extrapolated linearly to $\tau = 0$, whereas $\sigma_{\text{norm}} \propto \tau$ (inset). (b) At the longest lifetime, $\tau = 20$, a clear scaling collapse occurs: $\sigma_{\text{anom}} \propto \mu^2 + T^2 \pi^2 / 3$ with almost the precise prefactor in accordance with Eq. (10). We have used $\xi_{\mathbf{k}} = k^2/2 - 50$, $t_\perp = 10$ and $\delta t_{\mathbf{k}} = -5k_y/k$, which gives a semicircular FA along $k = 10$ for $k_y < 0$, and set $|e| = \hbar = k_B = 1$.

where $n_{\text{norm}} = \int_{\mathbf{k}} f(\xi_{\mathbf{k}} - \mu) W_{\mathbf{k}}$ and

$$n_{\text{anom}} = \int_{\mathbf{k}} \int_{BC} f(E) \frac{\text{sgn}(E + \mu) |b_{\mathbf{k}}|}{(t_\perp + \delta t_{\mathbf{k}})^2 (E + \mu - \xi_{\mathbf{k}})}. \quad (11)$$

As in the case of σ_{anom}, the integral receives contributions only from the regions near the Weyl nodes. Carrying out this integral by linearizing around the Weyl nodes as before, we get $n_{\text{anom}} = \sum_j n_{\text{anom},j}$, with

$$n_{\text{anom},j} = \frac{\mu(\mu^2 + k_B^2 T^2 \pi^2)}{6\pi^2 \hbar^3} \frac{c}{|(\mathbf{u}_j \times \mathbf{v}_j) \cdot \mathbf{w}_j|}. \quad (12)$$

This, in turn, gives an effective DOS from the BC, $\nu_{\text{anom},j} = dn_{\text{anom},j}/d\mu$, in terms of which Eq. (10) can be expressed as

$$\sigma_{\text{anom}} = \sum_j e^2 \nu_{\text{anom},j} v_{j,x}^2 \frac{2\hbar}{t_\perp}. \tag{13}$$

Written as above, σ_{anom} resembles the Drude conductivity of a 2D metal, similar to σ_{norm} in Eq. (8), except that the DOS on the FA is replaced by an effective DOS on the surface due to the bulk and $\tilde{\tau} = 2\hbar/t_\perp$ plays the role of lifetime in lieu of $\tau_{\mathbf{k}}$.

The appearance of a new effective lifetime can be traced to the fact that $\text{Im}G^R \neq 0$ when $E \in BC$ even when $1/\tau_{\mathbf{k}} = 0$. In fact, one can write Eq. (5) as

$$G_{\mathbf{k}}^R(E) = \frac{Z_{\mathbf{k}}(E)}{E + \mu - \xi_{\mathbf{k}} + \frac{i\hbar}{2\tilde{\tau}_{\mathbf{k}}(E)}},$$

$$Z_{\mathbf{k}} = \frac{a_{\mathbf{k}}(E)^2 + |b_{\mathbf{k}}(E)|^2}{2a_{\mathbf{k}}(E)(t_\perp + \delta t_{\mathbf{k}})^2}, \tag{14}$$

$$\frac{\hbar}{2\tilde{\tau}_{\mathbf{k}}(E)} = \text{sgn}(E + \mu)(E + \mu - \xi_{\mathbf{k}})\frac{|b_{\mathbf{k}}(E)|}{a_{\mathbf{k}}(E)},$$

in the region $|E + \mu| > E_{\mathbf{k}-}$. This resembles an interacting Green's function where $Z_{\mathbf{k}}(E)$ is the quasiparticle residue and $\tilde{\tau}_{\mathbf{k}}(E)$ is the effective lifetime. At a Weyl node at $E = 0$, we find $\tilde{\tau}_{\mathbf{k}}(0) = \hbar/4t_\perp$ which shows up as the scattering time in the anomalous contribution upto prefactors. Thus, the bulk states effectively induce an interacting 2D fluid on the surface near the Weyl nodes, leading to the additional anomalous contribution σ_{anom} on the surface.

V. EXPERIMENT

Our main results, Eqs. (1), (8), and (10), imply that the surface of a WSM, in spite of being a metal, exhibits a non-metallic signature in transport: The conductivity (resistivity) increases (decreases) with increase in T with a characteristic quadratic dependence. This can be studied experimentally to verify our theory. As an example we consider the commonly studied Weyl semimetal TaAs: For the W1 Weyl nodes, in-plane velocity $\approx 3 \times 10^5$ m/s, out-of-plane velocity $\approx 3 \times 10^4$ m/s, $\tau \sim 0.1$ps, $c \sim 10$Å, $v_F \sim 0.02$ eV^{-1}Å^{-2}, and $t_\perp \sim 0.01$eV [11,83]. This yields $\sigma_{\text{norm}} \sim 10^{-3}\Omega^{-1}$ and $\sigma_{\text{anom}}(T) - \sigma_{\text{anom}}(0) \sim 10^{-9}T^2\Omega^{-1}$K^{-2}, which evaluates to $\sim 10^{-7}\Omega^{-1}$ for $T \sim 10^1$K. A change in resistance of 1 part in 10^4 is easily measurable, implying that our predicted effect is readily amenable to experimental verification; a similar estimate can be obtained for other Weyl materials. In arriving at this, however, we assumed τ to be T independent in Eq. (8). In reality, this is not true—τ does depend on T and is, in fact, the chief source of T dependence in the σ_{norm}, which can compete with the T^2 dependence in σ_{anom}. Nevertheless, below a certain temperature T_D whose exact value will depend on the microscopics, the T dependence of σ_{surf} can be dominated by σ_{anom} even with a T-dependent τ. For example, if one assumes the usual form of electron-phonon scattering with the scattering time given by $\hbar/\tau_{e-ph} \sim k_B T^4/T_{BG}^3$, ($T_{BG}$ is the Bloch-Gruneisen temperature for the FA states), then $T_D \sim (\hbar k_B^{1/2}/\tau)(T_{BG}/t_\perp)^{3/2}$. For $T_{BG} \sim 100$ K and $t_\perp \sim 0.01$ eV, one gets $T_D \sim 65$ K. On the other hand, below an even lower temperature, say T_Q, quantum corrections, not
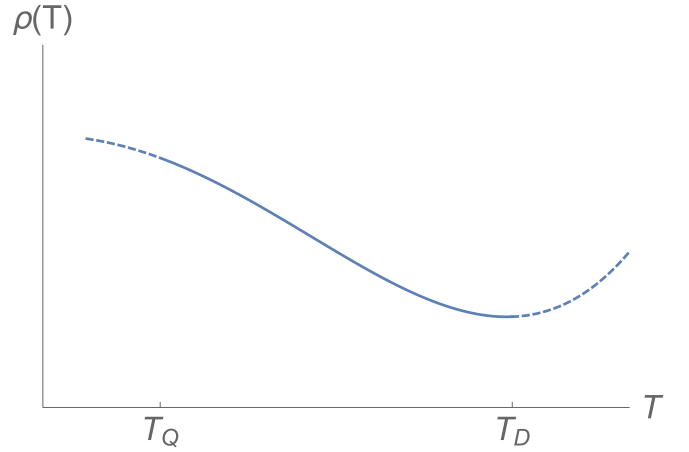

FIG. 3. Schematic depiction of the T dependence of the surface resistivity, $1/\sigma_{\text{surf}}$, according to Eq. (1). Above T_D, the T dependence of τ is significant whereas quantum corrections not considered in this work become important below T_Q. For $T_Q \lesssim T \lesssim T_D$, the resistivity is expected to grow quadratically with decreasing T due to σ_{anom}.

considered in this work, will become important. The predicted effect will, therefore, be observable for $T_Q \lesssim T \lesssim T_D$, and is illustrated in terms of resistivity in Fig. 3.

VI. DISCUSSION

The expression for the surface conductivity used in Eq. (6) considers electrons restricted to move along the top layer. Nevertheless, electrons on the surface can tunnel to other layers and reappear on the surface. Such processes also contribute to the surface conductivity, but have been ignored so far. Including these effects, however, does not change the qualitative results. As shown in SM [82], the τ and T dependences of σ_{norm} and σ_{anom} remain unchanged at low temperature and doping. The only consequence of these extra terms is a renormalization of $W_{\mathbf{k}}^2$ in σ_{norm}: $W_{\mathbf{k}}^2 \to \tilde{W}_{\mathbf{k}}^2 = W_{\mathbf{k}}^2/(1 - W_{\mathbf{k}}^2)$ in Eq. (7) while σ_{anom} in Eq. (10) receives corrections that are suppressed by powers of $|\mu|/t_\perp$ and $k_B T/t_\perp$.

Another aspect of our calculations that need scrutiny is that our starting model in Eq. (2) defines a WSM, which assumes the bilayer basis in real space to be identical to the band basis in energy space. In general, this need not be true. However, in such cases, the bilayer basis and the low-energy band basis can be related by a $\mathbf{k}$-dependent unitary transformation $U_{\mathbf{k}}$. In SM [82] we show that $U_{\mathbf{k}}$ does not modify the salient qualitative features σ_{surf}. This is essentially because $U_{\mathbf{k}}$ does not change the analytic structure of $G_{\mathbf{k}}(E)$, which continues to retain poles along the FAs and BCs within the bulk bands.

Finally, we note that, while σ_{surf} stems from topological features such as the FAs and inseparability of the surface from the bulk, the response itself is nontopological as it does not descend from a topological response theory. Indeed, as shown in SM [82], an ordinary metal also acquires a T^2 term in the surface conductivity. However, this term vanishes as the bulk Fermi surface shrinks to zero, in contrast to σ_{anom}, which is nonzero at finite T even when the Weyl nodes are undoped. Additionally, the μ and T dependences in ordinary metals are essentially unrelated whereas σ_{anom} only depends

on the combination $\mu^2 + k_B^2 T^2 \pi^2/3$ according to (10). Both these properties stem from the innate linear dispersion of Weyl fermions. In this sense, σ_{surf} is the surface counterpart of the bulk longitudinal conductivity that stems from topological Weyl fermions but is itself nontopological [26,84]. Nevertheless, it paves the way to search for other, possibly topological, surface responses to complement the extensively studied bulk topological responses originating from the Weyl nodes.

VII. CONCLUSION

We have shown that the dc surface conductivity of a WSM contains an anomalous contribution at nonzero temperature and doping in addition to the expected Drude contribution from the FAs. The novel contribution is manifestly non-Drude in character, being independent of the in-plane scattering time, stems from the intrinsic inseparability of the surface from the bulk, and dominates the temperature dependence at low temperatures. Moreover, its temperature and doping dependences are locked to each other by a universal, dimensionless ratio: $k_B^2 \pi^2/3$. We argued that the bulk states when projected on the surface mimic a correlated liquid, and the anomalous conductivity can be understood as a response of this liquid.

[1] O. Vafek and A. Vishwanath, Annu. Rev. Condens. Matter Phys. **5**, 83 (2014).

[2] A. A. Burkov, Annu. Rev. Condens. Matter Phys. **9**, 359 (2018).

[3] A. A. Burkov, Nature Mater. **15**, 1145 (2016).

[4] B. Yan and C. Felser, Annu. Rev. Condens. Matter Phys. **8**, 337 (2017).

[5] N. P. Armitage, E. J. Mele, and A. Vishwanath, Rev. Mod. Phys. **90**, 015001 (2018).

[6] S.-Q. Shen, *Topological Dirac and Weyl Semimetals* (Springer, Singapore, 2017), pp. 207–229.

[7] I. Belopolski, D. S. Sanchez, Y. Ishida, X. Pan, P. Yu, S.-Y. Xu, G. Chang, T.-R. Chang, H. Zheng, N. Alidoust, G. Bian, M. Neupane, S.-M. Huang, C.-C. Lee, Y. Song, H. Bu, G. Wang, S. Li, G. Eda, H.-T. Jeng, T. Kondo, H. Lin, Z. Liu, F. Song, S. Shin, and M. Z. Hasan, Nature Commun. **7**, 13643 (2016).

[8] Z. P. Guo, P. C. Lu, T. Chen, J. F. Wu, J. Sun, and D. Y. Xing, Sci. China Phys. Mech. Astron. **61**, 038211 (2018).

[9] G. Chang, S.-Y. Xu, H. Zheng, C.-C. Lee, S.-M. Huang, I. Belopolski, D. S. Sanchez, G. Bian, N. Alidoust, T.-R. Chang, C.-H. Hsu, H.-T. Jeng, A. Bansil, H. Lin, and M. Z. Hasan, Phys. Rev. Lett. **116**, 066601 (2016).

[10] A. Gyenis, H. Inoue, S. Jeon, B. B. Zhou, B. E. Feldman, Z. Wang, J. Li, S. Jiang, Q. D. Gibson, S. K. Kushwaha, J. W. Krizan, N. Ni, R. J. Cava, B. A. Bernevig, and A. Yazdani, New J. Phys. **18**, 105003 (2016).

[11] S.-M. Huang, S.-Y. Xu, I. Belopolski, C.-C. Lee, G. Chang, B. Wang, N. Alidoust, G. Bian, M. Neupane, C. Zhang, S. Jia, A. Bansil, H. Lin, and M. Z. Hasan, Nature Commun. **6**, 7373 (2015).

[12] H. Inoue, A. Gyenis, Z. Wang, J. Li, S. W. Oh, S. Jiang, N. Ni, B. A. Bernevig, and A. Yazdani, Science **351**, 1184 (2016).

[13] B. Q. Lv, N. Xu, H. M. Weng, J. Z. Ma, P. Richard, X. C. Huang, L. X. Zhao, G. F. Chen, C. E. Matt, F. Bisti, V. N. Strocov, J. Mesot, Z. Fang, X. Dai, T. Qian, M. Shi, and H. Ding, Nature Phys. **11**, 724 (2015).

[14] Y. Sun, S. C. Wu, and B. Yan, Phys. Rev. B **92**, 115428 (2015).

[15] S.-Y. Xu, I. Belopolski, N. Alidoust, M. Neupane, G. Bian, C. Zhang, R. Sankar, G. Chang, Z. Yuan, C.-C. Lee, S.-M. Huang, H. Zheng, J. Ma, D. S. Sanchez, B. Wang, A. Bansil, F. Chou, P. P. Shibayev, H. Lin, S. Jia, and M. Z. Hasan, Science **349**, 613 (2015).

[16] S. Y. Xu, I. Belopolski, D. S. Sanchez, M. Neupane, G. Chang, K. Yaji, Z. Yuan, C. Zhang, K. Kuroda, G. Bian, C. Guo, H. Lu, T. R. Chang, N. Alidoust, H. Zheng, C. C. Lee, S. M. Huang, C. H. Hsu, H. T. Jeng, A. Bansil, T. Neupert, F. Komori, T. Kondo, S. Shin, H. Lin, S. Jia, and M. Z. Hasan, Phys. Rev. Lett. **116**, 096801 (2016).

[17] L. X. Yang, Z. K. Liu, Y. Sun, H. Peng, H. F. Yang, T. Zhang, B. Zhou, Y. Zhang, Y. F. Guo, M. Rahn, D. Prabhakaran, Z. Hussain, S. K. Mo, C. Felser, B. Yan, and Y. L. Chen, Nature Phys. **11**, 728 (2015).

[18] H. Zheng, S. Y. Xu, G. Bian, C. Guo, G. Chang, D. S. Sanchez, I. Belopolski, C. C. Lee, S. M. Huang, X. Zhang, R. Sankar, N. Alidoust, T. R. Chang, F. Wu, T. Neupert, F. Chou, H. T. Jeng, N. Yao, A. Bansil, S. Jia, H. Lin, and M. Z. Hasan, ACS Nano **10**, 1378 (2016).

[19] P. Hosur and X. Qi, C. R. Phys. **14**, 857 (2013).

[20] H. Wang and J. Wang, Chin. Phys. B **27**, 107402 (2018).

[21] J. Hu, S.-Y. Xu, N. Ni, and Z. Mao, Annu. Rev. Mater. Res. **49**, 207 (2019).

[22] A. A. Zyuzin and A. A. Burkov, Phys. Rev. B **86**, 115133 (2012).

[23] Y. Chen, S. Wu, and A. A. Burkov, Phys. Rev. B **88**, 125105 (2013).

[24] M. M. Vazifeh and M. Franz, Phys. Rev. Lett. **111**, 027201 (2013).

[25] A. A. Burkov, J. Phys.: Condens. Matter **27**, 113201 (2015).

[26] P. Hosur, S. A. Parameswaran, and A. Vishwanath, Phys. Rev. Lett. **108**, 046602 (2012).

[27] F. de Juan, A. G. Grushin, T. Morimoto, and J. E. Moore, Nature Commun. **8**, 15995 (2017).

[28] S. Wang, B. C. Lin, A. Q. Wang, D. P. Yu, and Z. M. Liao, Adv. Phys.: X **2**, 518 (2017).

[29] K. Halterman, M. Alidoust, and A. Zyuzin, Phys. Rev. B **98**, 085109 (2018).

[30] K. Halterman and M. Alidoust, Opt. Express **27**, 36164 (2019).

[31] N. Nagaosa, T. Morimoto, and Y. Tokura, Nature Rev. Mater. **5**, 621 (2020).

[32] H. B. Nielsen and M. Ninomiya, Phys. Lett. B **130**, 389 (1983).

[33] M. V. Isachenkov and A. V. Sadofyev, Phys. Lett. B **697**, 404 (2011).

[34] A. V. Sadofyev, V. I. Shevchenko, and V. I. Zakharov, Phys. Rev. D **83**, 105025 (2011).

[35] R. Loganayagam and P. Surówka, J. High Energy Phys. 04 (2012) 097.

[36] P. Goswami and S. Tewari, Phys. Rev. B **88**, 245107 (2013).

[37] Z. Wang and S.-C. Zhang, Phys. Rev. B **87**, 161107(R) (2013).

[38] G. Başar, D. E. Kharzeev, and H.-U. Yee, Phys. Rev. B **89**, 035142 (2014).

[39] K. Landsteiner, Phys. Rev. B **89**, 075124 (2014).

[40] E. Benito-Matías and R. A. Molina, Phys. Rev. B **99**, 075304 (2019).

[41] P. Deng, Z. Xu, K. Deng, K. Zhang, Y. Wu, H. Zhang, S. Zhou, and X. Chen, Phys. Rev. B **95**, 245110 (2017).

[42] K. Deng, G. Wan, P. Deng, K. Zhang, S. Ding, E. Wang, M. Yan, H. Huang, H. Zhang, Z. Xu, J. Denlinger, A. Fedorov, H. Yang, W. Duan, H. Yao, Y. Wu, S. Fan, H. Zhang, X. Chen, and S. Zhou, Nature Phys. **12**, 1105 (2016).

[43] F. Haldane, arXiv:1401.0529.

[44] P. Hosur, Phys. Rev. B **86**, 195102 (2012).

[45] L. Huang, T. M. McCormick, M. Ochi, Z. Zhao, M. T. Suzuki, R. Arita, Y. Wu, D. Mou, H. Cao, J. Yan, N. Trivedi, and A. Kaminski, Nature Mater. **15**, 1155 (2016).

[46] D. Iaia, G. Chang, T.-R. Chang, J. Hu, Z. Mao, H. Lin, S. Yan, and V. Madhavan, npj Quantum Mater. **3**, 38 (2018).

[47] H. Kwon, T. Jeong, S. Appalakondaiah, Y. Oh, I. Jeon, H. Min, S. Park, Y. J. Song, E. Hwang, and S. Hwang, Nano Res. **13**, 2534 (2020).

[48] A. Lau, K. Koepernik, J. Van Den Brink, and C. Ortix, Phys. Rev. Lett. **119**, 076801 (2017).

[49] M. Sakano, M. S. Bahramy, A. Tsuji, I. Araya, K. Ikeura, H. Sakai, S. Ishiwata, K. Yaji, K. Kuroda, A. Harasawa, S. Shin, and K. Ishizaka, Phys. Rev. B **95**, 121101(R) (2017).

[50] S. Y. Xu, I. Belopolski, D. S. Sanchez, C. Zhang, G. Chang, C. Guo, G. Bian, Z. Yuan, H. Lu, T. R. Chang, P. P. Shibayev, M. L. Prokopovych, N. Alidoust, H. Zheng, C. C. Lee, S. M. Huang, R. Sankar, F. Chou, C. H. Hsu, H. T. Jeng, A. Bansil, T. Neupert, V. N. Strocov, H. Lin, S. Jia, and M. Zahid Hasan, Sci. Adv. **1**, 1501092 (2015).

[51] S. Y. Xu, C. Liu, S. K. Kushwaha, R. Sankar, J. W. Krizan, I. Belopolski, M. Neupane, G. Bian, N. Alidoust, T. R. Chang, H. T. Jeng, C. Y. Huang, W. F. Tsai, H. Lin, P. P. Shibayev, F. C. Chou, R. J. Cava, and M. Z. Hasan, Science **347**, 294 (2015).

[52] Q. Xu, E. Liu, W. Shi, L. Muechler, J. Gayles, C. Felser, and Y. Sun, Phys. Rev. B **97**, 235416 (2018).

[53] Y. Yuan, X. Yang, L. Peng, Z.-J. Wang, J. Li, C.-J. Yi, J.-J. Xian, Y.-G. Shi, and Y.-S. Fu, Phys. Rev. B **97**, 165435 (2018).

[54] Q.-Q. Yuan, L. Zhou, Z.-C. Rao, S. Tian, W.-M. Zhao, C.-L. Xue, Y. Liu, T. Zhang, C.-Y. Tang, Z.-Q. Shi, Z.-Y. Jia, H. Weng, H. Ding, Y.-J. Sun, H. Lei, and S.-C. Li, Sci. Adv. **5**, aaw9485 (2019).

[55] C. Zhang, A. Narayan, S. Lu, J. Zhang, H. Zhang, Z. Ni, X. Yuan, Y. Liu, J.-H. Park, E. Zhang, W. Wang, S. Liu, L. Cheng, L. Pi, Z. Sheng, S. Sanvito, and F. Xiu, Nature Commun. **8**, 1272 (2017).

[56] P. J. W. Moll, N. L. Nair, T. Helm, A. C. Potter, I. Kimchi, A. Vishwanath, and J. G. Analytis, Nature (London) **535**, 266 (2016).

[57] A. C. Potter, I. Kimchi, and A. Vishwanath, Nature Commun. **5**, 5161 (2014).

[58] Y. Zhang, D. Bulmash, P. Hosur, A. Potter, and A. Vishwanath, Sci. Rep. **6**, 23741 (2016).

[59] E. V. Gorbar, V. A. Miransky, I. A. Shovkovy, and P. O. Sukhachov, Phys. Rev. B **93**, 235127 (2016).

[60] J. H. Wilson, J. H. Pixley, D. A. Huse, G. Refael, and S. Das Sarma, Phys. Rev. B **97**, 235108 (2018).

[61] G. Resta, S.-T. Pi, X. Wan, and S. Y. Savrasov, Phys. Rev. B **97**, 085142 (2018).

[62] D. K. Mukherjee, D. Carpentier, and M. O. Goerbig, Phys. Rev. B **100**, 195412 (2019).

[63] M. Breitkreiz and P. W. Brouwer, Phys. Rev. Lett. **123**, 066804 (2019).

[64] M. Z. Hasan and C. L. Kane, Rev. Mod. Phys. **82**, 3045 (2010).

[65] X.-L. Qi and S.-C. Zhang, Rev. Mod. Phys. **83**, 1057 (2011).

[66] J. Borchmann and T. Pereg-Barnea, Phys. Rev. B **96**, 125153 (2017).

[67] C. M. Wang, H. P. Sun, H. Z. Lu, and X. C. Xie, Phys. Rev. Lett. **119**, 136806 (2017).

[68] Y. Zhang, Phys. Rev. Res. **1**, 022005(R) (2019).

[69] S. Nishihaya, M. Uchida, Y. Nakazawa, M. Kriener, Y. Taguchi, and M. Kawasaki, Nature Commun. **12**, 2572 (2021).

[70] C. Zhang, Y. Zhang, X. Yuan, S. Lu, J. Zhang, A. Narayan, Y. Liu, H. Zhang, Z. Ni, R. Liu, E. S. Choi, A. Suslov, S. Sanvito, L. Pi, H.-Z. Lu, A. C. Potter, and F. Xiu, Nature (London) **565**, 331 (2019).

[71] Ž. B. Lošić, J. Phys.: Condens. Matter **30**, 365003 (2018).

[72] O. V. Bugaiko, E. V. Gorbar, and P. O. Sukhachov, Phys. Rev. B **102**, 085426 (2020).

[73] E. V. Gorbar, V. A. Miransky, I. A. Shovkovy, and P. O. Sukhachov, Phys. Rev. B **99**, 155120 (2019).

[74] J. Hofmann and S. Das Sarma, Phys. Rev. B **93**, 241402(R) (2016).

[75] T. Tamaya, T. Kato, K. Tsuchikawa, S. Konabe, and S. Kawabata, J. Phys.: Condens. Matter **31**, 305001 (2019).

[76] J. C. W. Song and M. S. Rudner, Phys. Rev. B **96**, 205443 (2017).

[77] G. M. Andolina, F. M. D. Pellegrino, F. H. L. Koppens, and M. Polini, Phys. Rev. B **97**, 125431 (2018).

[78] F. Adinehvand, Z. Faraei, T. Farajollahpour, and S. A. Jafari, Phys. Rev. B **100**, 195408 (2019).

[79] S. Ghosh and C. Timm, Phys. Rev. B **101**, 165402 (2020).

[80] M. I. Katsnelson and K. S. Novoselov, Solid State Commun. **143**, 3 (2007).

[81] O. E. Obakpolor and P. Hosur, Phys. Rev. B **106**, L081112 (2022).

[82] See Supplemental Material at http://link.aps.org/supplemental/10.1103/PhysRevB.106.245410 for the derivation of the main results and supporting calculations to justify the approximations employed in the derivation.

[83] B. Ramshaw, K. A. Modic, A. Shekhter, Y. Zhang, E.-A. Kim, P. J. Moll, M. D. Bachmann, M. Chan, J. Betts, F. Balakirev *et al.*, Nature Commun. **9**, 2217 (2018).

[84] A. A. Burkov and L. Balents, Phys. Rev. Lett. **107**, 127205 (2011).